Interdiffusion of Low Molecular Weight Deuterated Polystyrene and Poly(methyl methacrylate)

T. E. Shearmur,* A. S. Clough, D. W. Drew, and M. G. D. van der Grinten

Department of Physics, University of Surrey, Guildford, Surrey GU2 5XH, England

R. A. L. Jones

Cavendish Laboratory, University of Cambridge, Cambridge CB3 0HE, England

Received March 25, 1996; Revised Manuscript Received July 24, 1996[⊗]

ABSTRACT: The interdiffusion of deuterated polystyrene (d-PS) and poly(methyl methacrylate) (PMMA) of molecular weights low enough to enable total miscibility is studied at temperatures slightly above the glass transitions of both components. From diffusion profiles obtained by nuclear reaction analysis a function is derived which accurately describes the observed concentration dependence of the mutual diffusion coefficient. This function is compared to the predictions of the "slow" and "fast" theories of diffusion and is found to describe a thermal transition region between the two theories. Tracer diffusion coefficients are seen to vary with temperature according to the WLF equation but do not scale according to the Rouse theory. This is probably due to the narrow ranges of polymer molecular weights and temperatures studied.

I. Introduction

Polymer interdiffusion is of great importance for the production of new polymeric systems where interfaces play a key role. This is the case of the technologically significant areas of polymer welding and coating where the fusion and adhesion processes are critical to the final stability of the system.[1,2] The thermodynamic interactions between the polymers govern the rate at which the macroscopic composition gradients relax and the width of the interface between the two constituents. The properties of a system's interface, such as resistance to fracture, are strongly dependent on both these quantities. The study of such systems, whether leading directly to technologically useful interfaces or not, is required to test our knowledge and models of diffusion mechanisms.

Interdiffusion work has centered around two phenomena. "Thermodynamic slowing down" is expected to occur in the vicinity of the critical blend composition ϕ_c, where it was discovered that, at a given temperature, proximity to the binodal curve reduced the diffusion coefficient.[3,4] Other work has concentrated on whether the mutual diffusion coefficient can be described by some weighted average of the intrinsic chain mobilities of the individual components of a system, and if so, how that average is constructed. It is important to note there is no thermodynamic justification for the existence of such a relationship, so that any expression must contain certain physical assumptions. The "slow" theory,[5,6] is derived from a dynamic version of the random phase approximation and assumes local incompressibility, whereas the "fast" theory[7,8] assumes that local density inhomogeneities can exist, but are rapidly relaxed. Most interdiffusion data in the literature,[9−13] collected above T_g, are consistent with the fast theory where the faster diffusing component dominates diffusion and swells the slower component. However, when one or both polymers are below T_g, free volume effects become important and recent results[14−16] have shown systems with highly asymmetric diffusion profiles which cannot be described by either the fast or the slow theories.

Blends of polystyrene (PS) and poly(methyl methacrylate) (PMMA) have been studied for many years.[17−28] Stockmeyer and Stanley[17] performed light scattering experiments on ternary solutions of PS/PMMA/butanone to determine the Flory−Huggins interaction parameter (χ) between the two polymers in solution. This technique was then refined by Fukada and Inagaki[18,19] using an "inert" solvent of bromobenzene and by Su and Fried[20] who developed a theory to account for free volume effects. More recently small angle neutron scattering (SANS),[21−23] small angle X-ray scattering (SAXS),[24] neutron reflectometry,[25] and ellipsometry[26] have been used to measure the interfacial thickness between the undiluted polymers. χ was then determined from equations derived from the self-consistent field theory.[29,30] Cloud point measurements to determine the phase diagrams with various molecular weights have also been performed.[27,28] Comparing these diagrams to predictions from the Flory−Huggins[31] and other theories taking polymer compressibilities into consideration[32−34] also yields values for χ.

Many publications on PS/PMMA blends have determined χ, but results have been contradictory and the scattering of the values severely limits their practical use. Consensus is only obtained for molecular weights above several thousand grams for which all values agree on the immiscibility of the undiluted polymers.

This study looks at the mutual diffusion of deuterated polystyrene (d-PS) into PMMA at temperatures slightly above the glass transitions of both polymers. From the diffusion profiles obtained, diffusion coefficients were determined and a function derived which follows the data accurately. The function is then compared to the slow and fast theory predictions.

Diffusion profiles are obtained by nuclear reaction analysis (NRA). This is a technique which has been used for many years in the surface analysis of materials[35−37] but only recently[38,39] has it been applied to polymer studies. It is a straightforward nondestructive measurement technique enabling good depth profiling (up to 8 μm with a resolution of 400 nm using a 2 MeV beam normal to the sample surface) and resolution

[⊗] Abstract published in *Advance ACS Abstracts,* September 15, 1996.

S0024-9297(96)00458-5 CCC: $12.00

Table 1. Polymers Used in This Work

polymer type	designation	mol wt	T_g (°C)	M_w/M_n
PMMA	PMMA 3.1k	3100	72	1.07
PMMA	PMMA 4.7k	4700	84	1.09
d-PS	d-PS 4.5k	4550	73	1.04

(down to 15 nm using a 0.7 MeV beam at a glancing angle of 15°).

II. Experimental Section

The polymers used are described in Table 1. All polymers were supplied by Polymer Laboratories Ltd. and are monodisperse. The glass transitions are determined by DSC using a Perkin-Elmer DSC7 at a heating rate of 10 °C min^{-1}. They are consistently 10 °C lower than values interpolated between the T_g's measured by Callaghan and Paul[28] (at twice the heating rate) for polymers of similar molecular weights, also purchased from Polymer Laboratories Ltd. Samples are made by spin casting a film (≈0.5 μm thick) of PMMA onto an etched silicon wafer surface, from a toluene solution. The wafer is etched in buffered hydrofluoric acid (7:1) to prevent dewetting when annealed above T_g. A d-PS film (≈0.25 μm) is spin cast onto a glass microscope slide before being floated off onto distilled water and being picked up on the previously coated silicon wafer, thereby creating a bilayer. After the samples are left to dry overnight, annealing is performed in a vacuum oven at pressures of ≈10^{-1} Torr. Samples containing PMMA 3.1k are annealed at temperatures of 96, 105, 116, and 130 °C (±1 °C) and those containing PMMA 4.7k at temperatures of 114, 116, 124, and 135 °C. NRA is performed at the University of Surrey using a 2 MeV Van de Graaff accelerator as described previously.[38] The incident beam energy used is 0.7 MeV, and the angle of incidence is 30°. This enables a depth of ≈1 μm to be profiled with a resolution of 25 nm. Due to the high thermal sensitivity of PMMA, the samples are back-cooled with liquid nitrogen and the beam current is maintained at a low level (≈1 nA) to minimize damage. Spectra are typically obtained in 15 min, and sample examination after exposure to the beam and spectra reproducibility show that damage is avoided.

III. Theory

Flory−Huggins. According to the Flory−Huggins theory,[31] stability in a miscible polymer blend is achieved if the second derivative of the free energy of mixing (ΔG) with respect to ϕ_1 (the volume fraction of polymer 1) is positive:

$$\frac{1}{k_B T}\frac{\partial^2 \Delta G}{\partial \phi_1^{\,2}} = \frac{1}{N_1\phi_1} + \frac{1}{N_2\phi_2} - 2\chi > 0 \qquad (1)$$

where χ is the Flory−Huggins interaction parameter. For low molecular weight polymers the combinatorial entropy of mixing becomes significant and miscibility can be obtained for values of χ which are small and positive, as is the case for blends of PS and PMMA at temperatures between 100 and 200 °C.[18−28] The minimum value of χ on the spinodal, the line of instability of the blend, is found to be

$$\chi_{spc} = \frac{1}{2}\left(\frac{1}{\sqrt{N_1}} + \frac{1}{\sqrt{N_2}}\right)^2 \qquad (2)$$

This value depends only on the molecular weights of the polymers used and can be determined for any known system. The critical temperature (T_c) of the system, above which the polymers are perfectly miscible in all proportions, can be calculated if the temperature dependence of χ is known.

Diffusion. Diffusion in polymers above their T_g is governed by Fick's law. In one dimension, this is[40]

$$\frac{\partial \phi}{\partial t} = \frac{\partial}{\partial x}\left(D\frac{\partial \phi}{\partial x}\right) \qquad (3)$$

where t is time and D is the diffusion coefficient. For a constant D, the solution to this equation for a thin film diffusing into a semi-infinite medium is given by

$$\phi(x) = \frac{1}{2}(\phi_1 - \phi_2)\left[\mathrm{erf}\left(\frac{h-x}{w}\right) + \mathrm{erf}\left(\frac{h+x}{w}\right)\right] + \phi_2 \qquad (4)$$

where h is the thickness of the initial thin film and w is the characteristic depth of diffusion defined as $w = (4Dt)^{1/2}$. ϕ_1 and ϕ_2 are the initial concentrations of the profiled polymer in the thin top layer and thicker bottom layer, respectively. In the case of a concentration dependent diffusion coefficient, eq 3 cannot be solved analytically; unless the difference between ϕ_1 and ϕ_2 is small enough that D may be considered constant in that range, eq 3 must be solved numerically.

Fast Theory. The fast theory of diffusion[7,8] considers that when diffusion occurs in a binary polymer melt, the faster moving species seeks to penetrate the slower moving one. However, a flux of molecules in one direction only would raise the local density to an unacceptable level. A flux of the slower molecules must therefore occur in the opposite direction. The slower molecules, being too sluggish to relax the density by diffusion, do so by the faster mechanism of bulk flow. Using the Onsager formalism and Flory−Huggins theory, the interdiffusion of chemically different polymers of different molecular weights below their entanglement lengths is given by

$$D_F = [D^*_A N_A(1-\phi) + D^*_B N_B \phi]\left[\frac{1-\phi}{N_A} + \frac{\phi}{N_B} + \phi(1-\phi)\left|\chi\right|\right] \qquad (5)$$

where D^*_A and D^*_B are the tracer diffusion coefficients of the A and B segments according to the Rouse theory, such that

$$D^*_A = \frac{k_B T}{\zeta_A N_A} \qquad (6a)$$

and

$$D^*_B = \frac{k_B T}{\zeta_B N_B} \qquad (6b)$$

where ζ_A and ζ_B are the monomeric friction coefficients of the A and B polymers, respectively.

Slow Theory. The slow theory of diffusion[5,6] considers that density inhomogeneities do not occur; the fluxes of the diffusing species are therefore equal and opposite. In a way similar to the fast theory, the mutual diffusion coefficient is then found to be

$$D_S = \left[\frac{(1-\phi)}{D^*_A N_A} + \frac{\phi}{D^*_B N_B}\right]^{-1}\left[\frac{1-\phi}{N_A} + \frac{\phi}{N_B} + \phi(1-\phi)\left|\chi\right|\right] \qquad (7)$$

where all symbols have the same meaning as above and

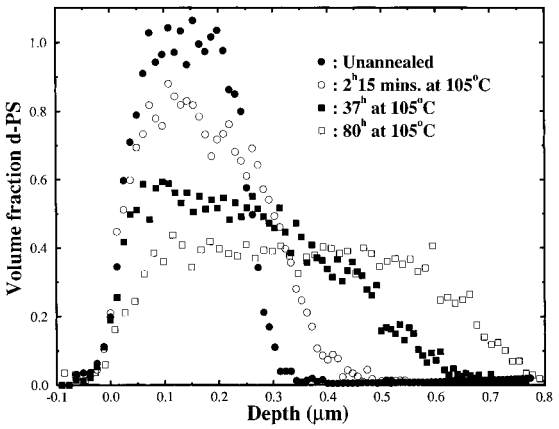

Figure 1. Typical set of diffusion profiles showing the swelling effect, the Fickian tail, and the uniform, equilibrium situation. These profiles were obtained from the PMMA 3.1k system.

the tracer diffusion coefficients of both components can be dependent on blend concentration.[41]

IV. Results and Discussion

A typical set of diffusion profiles is shown in Figure 1. At equilibrium (after many hours of annealing) the profile is uniform with the relative concentrations of d-PS and PMMA dependent only on the relative thickness of the two initial layers in the sample. This implies that the two polymers are perfectly miscible in all proportions and consequently that annealing was carried out above T_c. For the two systems studied here, χ_{spc} was calculated to be 0.057 and 0.046 for the PMMA 3.1k and 4.7k systems, respectively. According to Stühn[24] and Kressler[27] these values would correspond to critical temperatures well over 200 °C. Annealing around 100 °C would therefore be deep in the two phase region, and equilibrium would show a step function with the concentrations at both plateaus determined by the binodal.[42] According to Russell[22] and Callaghan and Paul,[28] these χ_{spc} values indicate T_c's well below −100 °C. Annealing around 100 °C is then clearly in the single phase region, which corresponds to our observations. Consistency with Callaghan and Paul's results is not surprising since both experiments were carried out with monodisperse homopolymers of similar molecular weights, purchased from the same supplier. We shall therefore use their value of χ in subsequent calculations.

$$\chi = 0.0202 + \frac{3.06}{T} \tag{8}$$

(χ is extracted from their value of Λ, the interaction energy density.)

With time, the initial profile broadens while a Fickian tail appears in front of the moving interface. Equation 4 is used to fit the tail part of the diffusion profiles (using $\phi_1 = 1$ and $\phi_2 = 0$, and letting h vary as a fitting parameter to exclude the swelling effect). The diffusion coefficients obtained from the fits are shown in Table 2. These coefficients have a strong temperature dependence and so we write the Williams−Landel−Ferry (WLF) equation[43] relating the diffusion coefficients at different temperatures:

$$\ln\left(\frac{D_T T_0}{D_{T_0} T}\right) = \frac{c_1^0 (T - T_0)}{T - T_\infty} \tag{9}$$

Table 2. Diffusion Coefficients Obtained from the Profile "Tails"

system	T (°C)	D (cm^2 s^{-1})
PMMA 3.1k	96	1.86×10^{-16}
	105	1.91×10^{-15}
	116	1.92×10^{-14}
	130	6.00×10^{-13}
PMMA 4.7k	114	5.06×10^{-16}
	116	1.73×10^{-15}
	124	7.41×10^{-15}
	135	9.82×10^{-14}

where D_T and D_{T_0} are the diffusion coefficients at temperatures T and T_0 (some arbitrary reference temperature), respectively, c_1^0 is a constant dependent on the monomeric friction coefficient, and T_∞ is the Vogel temperature, T_∞ is usually constant for a given polymer, but for low molecular weight polymers T_g has a sharp temperature dependence and T_∞ must vary accordingly.[44] Plotting $\ln(D_{T_0}T/D_T T_0)$ against $(T - T_0)/(T - T_\infty)$ for both the PMMA 3.1k and 4.7k systems with $T_\infty = T_g - 80$ °C,[43] yields straight lines with slopes (c_1^0) of 28.4 and 32.6 (cf. 34[43]), respectively, and shows that D, for both systems, scales as expected. However, one would expect these two values to be equal, indicating identical temperature dependencies of the tracer diffusion coefficients. These values imply that the Rouse model (which predicts tracer diffusion coefficients inversely proportional to the PMMA molecular weight) is not verified. The difference between the two values can be attributed to experimental error over the relatively small temperature range studied here.

The diffusion coefficient describing the mobilities of d-PS and PMMA appears to be composed of two parts which, within experimental error, may be separated and studied individually. One part is heavily concentration dependent and causes the d-PS to swell, the other is concentration independent (at least to a first approximation), varying with temperature according to the WLF equation predictions. Each part is dominant over a substantial concentration range.

These observations suggest the following functional form for the concentration dependence of the diffusion coefficient.

$$D_f = D_0 \quad \text{for} \quad \phi_{d-PS} < \phi_c \tag{10a}$$

$$D_f = D_0 + D_1(\exp[A(\phi - \phi_c)] - 1) \quad \text{for} \quad \phi_{d-PS} > \phi_c \tag{10b}$$

where D_0 is the diffusion coefficient determined earlier and ϕ_c is a temperature dependent critical concentration, marking the boundary between the two parts of D. The values of D_1 and A are constant at all temperatures for a given system and their significance will be discussed later. The diffusion coefficients for both systems at the various annealing temperatures are shown in Figure 2a,b. All the diffusion coefficients, except for the PMMA 3.1k samples annealed at 130 °C, were obtained from eqs 10a and 10b. For the PMMA 3.1k samples annealed at 130 °C eqs 10a and 10b do not apply because at this temperature ϕ_c would be smaller than 0. These samples will be discussed later. Using the method of finite differences[40] with these diffusion coefficients, numerical solutions to eq 3 are obtained. The resulting profiles are compared to the data, and excellent agreement is obtained for both systems at all temperatures and annealing times, as shown in Figure 3. This function was further tested

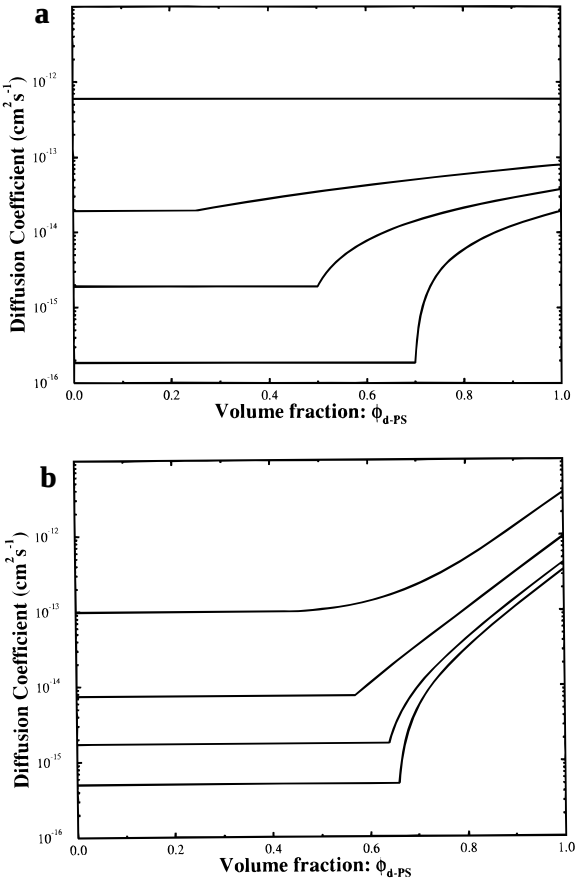

Figure 2. Diffusion coefficient against volume fraction, calculated from our function and used to obtain the numerical solutions to equation 3(a) for the PMMA 3.1k system at 96, 105, 116, and 130 °C (for 130 °C our function does not apply) and (b) for the PMMA 4.7k system at 114, 116, 124, and 135 °C.

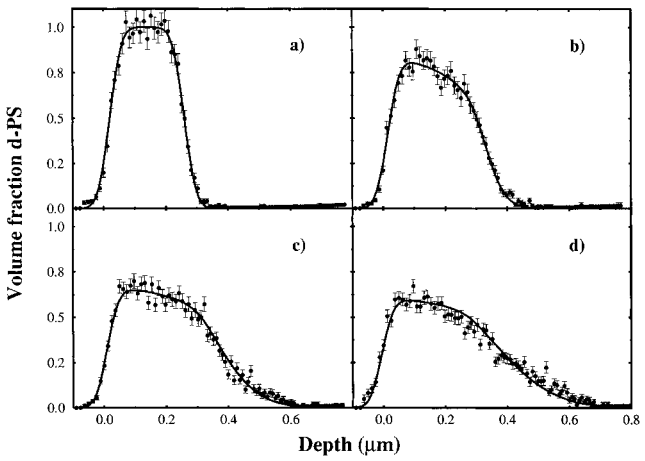

Figure 3. Comparison of the numerical solutions to the data obtained with the PMMA 3.1k system at 105 °C from samples annealed for various lengths of time; (a) unannealed sample (b) 135 min; (c) 540 min; (d) 960 min. The number of loops performed in the program calculating the numerical solution is directly proportional to the annealing time of the samples: 1 s = 3.05 loops (540 min = 98 680 loops).

by making bilayers with a top layer having an initial concentration in d-PS of ϕ_c and a bottom layer of pure PMMA; these profiles would then be expected to be Fickian in form, described by a single diffusion coefficient. The diffusion profiles obtained after annealing are fitted with eq 4 (using $\phi_1 = \phi_c$ and $\phi_2 = 0$) and are shown in Figure 4. For the PMMA 4.7k system at 124 °C, the diffusion coefficient obtained is 7.13×10^{-15} cm^2 s^{-1} (average from six samples), to be compared with 7.41×10^{-15} cm^2 s^{-1} obtained previously from fits to the tails of the nonblended bilayers.

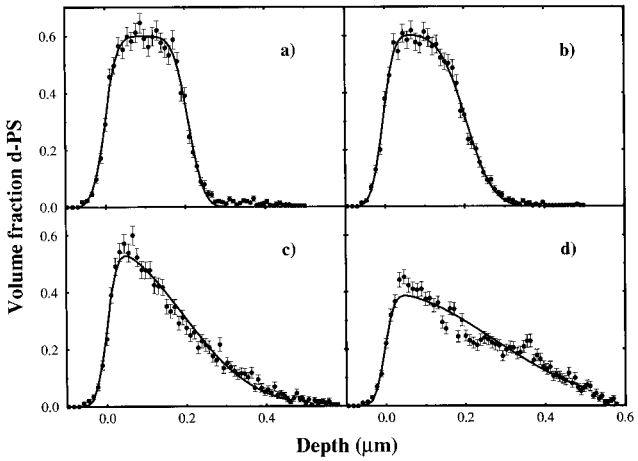

Figure 4. Depth profile obtained with the PMMA 4.7k system at 124 °C from samples made with a top layer containing a volume fraction $\phi = \phi_c = 0.57$ of d-PS and annealed for various lengths of time: (a) unannealed sample (b) 22 min; (c) 210 min; (d) 570 min. The solid lines are the best fits to the data obtained from eq 4, from which the diffusion coefficient is calculated.

Table 3. Tracer Diffusion Coefficients for PMMA in d-PS (D^*_{PMMA}) Calculated from Our Function Using Equations 10a and 10b

system	T (°C)	D^*_{PMMA} (cm^2 s^{-1})
PMMA 3.1k	96	1.94×10^{-14}
	105	3.76×10^{-14}
	116	8.07×10^{-14}
	130	6.00×10^{-13}
PMMA 4.7k	114	3.49×10^{-13}
	116	4.73×10^{-13}
	124	9.58×10^{-13}
	135	3.75×10^{-12}

Using our function, we then calculate the tracer diffusion coefficients of the PMMA into d-PS ($D^*_{PMMA} = D_f$ for $\phi_{d-PS} \rightarrow 1$). These values are shown in Table 3. As for D^*_{d-PS}, the values of D^*_{PMMA} are scaled according to the WLF equation. Again straight lines were obtained and values of c_1^0 were found to be 6.3 and 12.0 for the PMMA 3.1k and 4.7k systems, respectively. Despite the obvious uncertainty in these extrapolated values, they do appear to have some reliability: their values lead to accurate numerical solutions fitting the data and their temperature dependence is close to the $c_1^0 = 13$ tabulated in ref 43. These c_1^0 are much smaller than those obtained for the d-PS, indicating a much smaller temperature dependence of the PMMA tracer diffusion coefficients.

We can make another check of the constancy of the diffusion coefficient over the range of ϕ_{d-PS} from 0 to ϕ_c by determining the interdiffusion coefficient over a narrow range of concentrations, using diffusion couples with small concentration differences. Bilayers are made with a top layer containing 5% of d-PS and 95% PMMA 4.7k, placed on a matrix layer of pure PMMA 4.7k and annealed at 124 °C. Fitting the depth profiles obtained with eq 4 (using $\phi_1 = 0.05$ and $\phi_2 = 0$) gives a diffusion coefficient of 3.30×10^{-15} cm^2 s^{-1} for $\phi_{d-PS} = 0.025$. To determine the diffusion coefficient at $\phi_{d-PS} = 0.5$, bilayers are made with a top layer of 60% d-PS and 40% PMMA 4.7k and a matrix layer of 40% d-PS and 60% PMMA 4.7k. Here the diffusion coefficient is found to

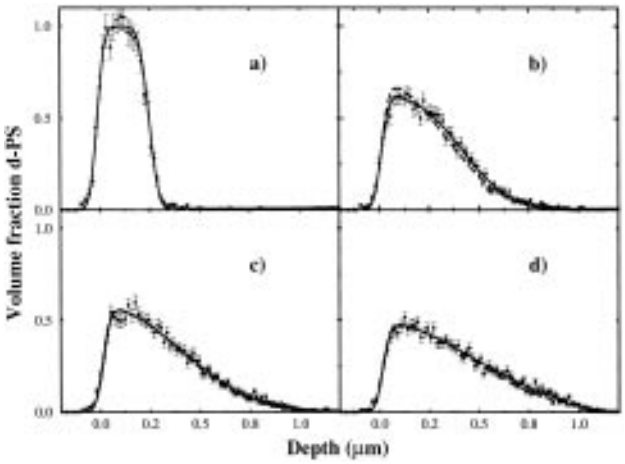

Figure 5. Depth profiles obtained with the PMMA 3.1k system at 130 °C from samples annealed for various lengths of time: (a) unannealed sample; (b) 6 min; (c) 10 min; (d) 15 min. The dashed lines are the numerical solutions obtained from the fast/slow modes using $D^*_{d-PS} = D^*_{PMMA}$ and the solid lines are best fits to the data using a simple Fickian model.

be 8.87×10^{-15} cm^2 s^{-1} for $\phi_{d-PS} = 0.5$ ($<\phi_c$). These values are to be compared with 7.13×10^{-15} cm^2 s^{-1} obtained previously, where the constant is therefore an averaged value over the concentration range below ϕ_c. These results do not invalidate those presented previously because the factor of 3 difference found in D_{d-PS} between $0 < \phi_{d-PS} < \phi_c$ over a concentration range of 0.5 is insignificant compared to the factor of ≈100 found between $\phi_c < \phi_{d-PS} < 1$ over the same concentration range. However these results will help in the comparison of our model with slow and fast theories.

We now discuss the extent to which our observations can be accounted for by either the fast or the slow theory. From the values of c_1^0 determined earlier from the WLF equation, we find that $D^*_{d-PS} = D^*_{PMMA}$ at temperatures of 130 and 181 °C for the PMMA 3.1k and 4.7k systems, respectively. This was indeed observed for the PMMA 3.1k system, where it was also noted that our function no longer applied because ϕ_c would be smaller than 0. In a system in which the tracer diffusion coefficients of both components (A and B) are independent of concentration, and at a temperature where $D^*_A = D^*_B$, the fast and slow theory predictions are identical and are very close to simple Fickian diffusion (for moderate χ). Figure 5 shows profiles obtained from the PMMA 3.1k system annealed at 130 °C for various lengths of time. The solid lines represent fast/slow theory numerical solutions to eq 3 and the dashed lines are Fickian fits to the data (using eq 4 with $\phi_1 = 1$ and $\phi_2 = 0$). Excellent agreement is obtained for all three diffusion modes with a diffusion coefficient $D^*_{d-PS} = D^*_{PMMA} = D_{mutual} = 6 \times 10^{-13}$ cm^2 s^{-1}. This result suggests (but does not prove) that the tracer diffusion coefficients of both components in our system are independent of concentration, and we shall assume that this is the case for the following discussion. This assumption is thought to be valid provided the T_g of the blend does not vary greatly with composition[5,7] (as is the case here). This has been verified experimentally in blends of unentangled poly(ethylene oxide) (PEO) and poly(propylene oxide) (PPO)[45] as well as in blends of unentangled poly(dimethylsiloxane) (PDMS) and poly(ethylmethylsiloxane) (PEMS).[46]

Assuming a linear concentration dependence of D_{d-PS} between $\phi = 0$ and $\phi = \phi_c$, Figure 6 shows D_f against

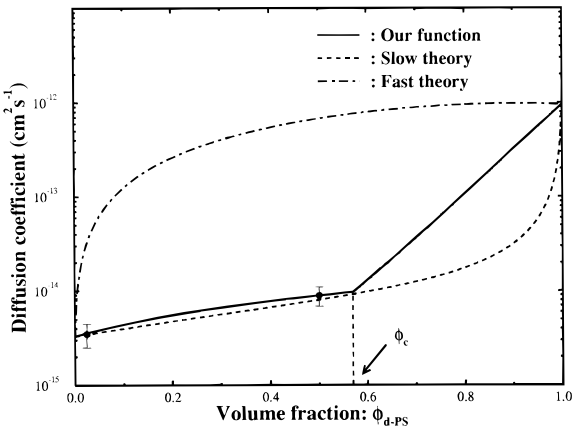

Figure 6. Plot of the diffusion coefficients predicted by the slow and fast theories and calculated from our function. The tracer diffusion coefficients (at $\phi = 0$ and 1) were measured (for D^*_{d-PS}) and calculated using our function (for D^*_{PMMA}). The curves are for the PMMA 4.7k system at 124 °C, and the plotted points are the coefficients measured at $\phi = 0.025$ and 0.5. The discontinuity in our function marks the location of ϕ_c.

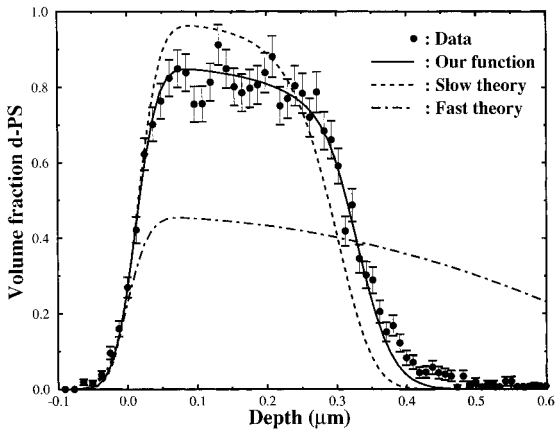

Figure 7. Comparison of the data with the numerical solutions using the slow and fast theories and our function. The data shown here was obtained from the PMMA 4.7k system annealed for 20 min at 124 °C. The number of loops performed in the program calculating each numerical solution is 20 min = 3655 loops.

ϕ_{d-PS}, as well as the slow and fast theory predictions determined from eqs 5 and 7. For these predictions D^*_{d-PS} is the measured value and D^*_{PMMA} the calculated value using eqs 10a and 10b. χ is determined from eq 8. Clearly for this system the fast theory does not apply. The slow theory, however, shows very good agreement between ϕ_c but serious deviations above ϕ_c. Allowing χ to vary within the limits of the values published in refs 18−28 has little effect on the shape of these curves. Figure 7 shows a spectrum compared with numerical solutions using slow and fast theories as well as our function. As expected from Figure 6, the fast theory shows very poor agreement with the data. Agreement can be improved by reducing the value of D^*_{PMMA} used in the fast theory. However, the profiles thus obtained clearly show that the diffusion coefficient is too small at high concentrations and too large at lower concentrations. The slow theory, although showing reasonable agreement, nevertheless presents significant deviations from the data; altering D^*_{PMMA} has very little effect on the slow theory numerical solutions. It is expected that at longer annealing times, agreement between the slow theory and the data will increase, due to the overall

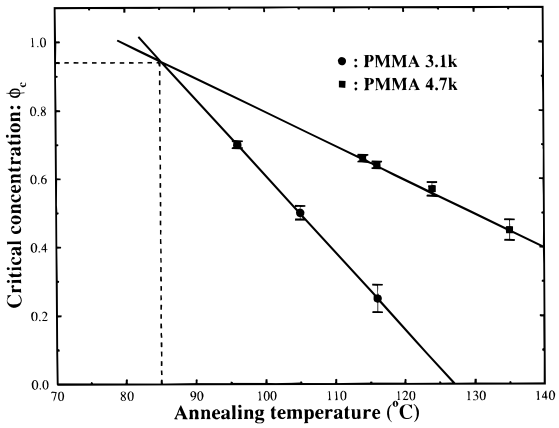

Figure 8. Plot of the critical concentration ϕ_c against temperature with the best straight line fits to the data. The lines are seen to intersect at $T = 85$ °C below which the slow theory is thought to dominate.

drop in concentration and consequent convergence of diffusion coefficients.

Thus it is clear that our results cannot be accounted for by either the slow theory or the fast theory. Below a critical concentration ϕ_c the interdiffusion coefficient varies rather slowly; thus there is a range of concentrations over which the interdiffusion coefficient is dominated by the slowest diffusing component, as predicted by the slow theory. However, above this critical concentration the interdiffusion coefficient rapidly rises toward the fast theory limit. We now consider what physical significance can be attached to the parameters in our function.

It was mentioned earlier that both D_1 and A were constants at all temperatures for a given system. D_1 appears to be proportional to the PMMA molecular weight. There seems to be a correlation between the magnitude of A and the difference in glass transition temperatures between the two polymers; for the PMMA 4.7k system, the difference in glass transition temperatures is 11 °C, and the value of A is about 10 times greater than in the other system, where the difference in glass transition temperature is 1 deg.

Finally, the values of ϕ_c are shown in Figure 8, where the errors are estimates determined by the closeness of the numerical solutions to the data. ϕ_c is seen to vary linearly with temperature, but the variation depends on the molecular weight of the PMMA. The best line fits to both sets of data intersect at $T = 85$ °C and $\phi_c = 0.95$. This indicates that as annealing temperature is decreased, ϕ_c will tend to 1 and, according to our function, D_f will tend to $D_0 = D_S$. Figure 8 seems to indicate that at temperatures below 85 °C ($\approx$10 deg above T_g) the slow theory would apply. Annealing at higher temperatures, where $\phi_c = 0$, would then be dominated by the exponential term of our model. It is then conceivable that at high enough temperatures the interdiffusion would follow the fast theory predictions. This is similar to the findings of Akcasu *et al.*[47] who by defining vacancies as the third component in a mixture of A and B polymers while analyzing the two exponential decay modes in dynamic scattering from ternary polymer solutions, concluded that the slow theory was obtained when the vacancies were removed (*i.e.* below T_g) and the fast theory obtained in the limit of high vacancy concentration (*i.e.* above T_g). Here we find that the changeover between fast and slow theories occurs gradually over a temperature range which depends on the polymer molecular weights (between 50 and 100 °C for the polymers used in this work) and begins 10 deg above T_g. These results are in contradiction with the relation recently developed by Brereton,[48] which predicts fast theory diffusion as a limit at low temperatures and slow theory diffusion at higher temperatures,[49] but are consistent with diffusion data obtained by Feng *et al.*[50] in PS/PVME blends.

The experiments suggested above to test the predictions of our function are currently being performed. However, it is evident from the results of Figure 5 that $\phi_c = 0$ is not a sufficient condition to observe fast mode diffusion; there must also be a significant difference between the tracer diffusion coefficients of both components.

V. Summary

The interdiffusion of deuterated polystyrene and poly(methyl methacrylate) of molecular weights low enough to enable total miscibility was studied at a variety of annealing temperatures above the glass transition temperatures (T_g) of the individual polymers. The tracer diffusion coefficients of each component seemed to be independent of concentration, which is possible for blends of polymers having similar T_g's. The diffusion profiles obtained by nuclear reaction analysis were shown not to agree with either the fast or slow mode predictions. A function was derived to describe the concentration dependence of the mutual diffusion coefficient from which numerical solutions to Fick's diffusion equation were obtained. These were compared to the diffusion profiles observed at all annealing temperatures and found to be accurate. This function indicates that at low enough temperatures the diffusion would occur following the slow theory and at high enough temperatures the fast theory would dominate. The function therefore seems to describe a thermal transition region between the two accepted theories, and experimental work is being carried out to test these predictions. The tracer diffusion coefficients were seen to follow the WLF equation but did not scale according to the inverse of their molecular weight, as the Rouse theory predicts. This is thought to be due to experimental error caused by looking at narrow ranges of polymer molecular weights and temperature.

References and Notes

(1) Tirrell, M. *Rubber Chem. Technol.* **1984**, *57*, 523−56.
(2) Brochard-Wyart, F. In *Fundamentals of Adhesion*; Lee, T. D., Ed.; Plenum: New York, 1988.
(3) Green, P. F.; Doyle, B. L. *Phys. Rev. Lett.* **1986**, *57*, 2407.
(4) Green, P. F.; Doyle, B. L. *Macromolecules* **1987**, *20*, 2471.
(5) Brochard-Wyart, F.; Jouffroy, J.; Levinson, P. *Macromolecules* **1983**, *16*, 1638.
(6) Binder, K. *Chem. Phys.* **1983**, *79*, 6387.
(7) Kramer, E. J.; Green, P.; Palmstrøm, C. J. *Polymer* **1984**, *25*, 473.
(8) Sillescu, H. *Makromol. Chem., Rapid Commun.* **1984**, *5*, 519.
(9) Jones, R. A. L.; Klein, J.; Donald, A. M. *Nature* **1986**, *321*, 161.
(10) Jordan, E. A.; Ball, R. C.; Donald, A. M.; Fetters, L. J.; Jones, R. A. L.; Klein, J. *Macromolecules* **1988**, *21*, 235.
(11) Composto, R. J.; Meyer, J. W.; Kramer, E. J.; White, D. M. *Phys. Rev. Lett.* **1986**, *57*, 1312.
(12) Composto, R. J.; Kramer, E. J.; White, D. M. *Nature* **1987**, *328*, 234.
(13) Kausch, H. H.; Tirrell, M. *Annu. Rev. Mater. Sci.* **1989**, *19*, 341.
(14) Sauer, B. B.; Walsh, D. J. *Macromolecules* **1991**, *24*, 5948.
(15) Jabbari, E.; Peppas, N. A. *Macromolecules* **1993**, *26*, 2175.
(16) Jabbari, E.; Peppas, N. A. *Polymer* **1995**, *36*, 575.
(17) Stockmeyer, W. H.; Stanley, H. E. *J. Chem. Phys.* **1950**, *18*, 153.
(18) Fukada, T.; Inagaki, H. *Pure Appl. Chem.* **1983**, *55*, 1541.

(19) Fukada, T.; Nagata, M.; Inagaki, H. *Macromolecules* **1986**, *19*, 1411.
(20) Su, A. C.; Fried, J. R. *Macromolecules* **1986**, *19*, 1417.
(21) Benoit, H.; Wu, W.; Benmouna, M.; Mozer, B.; Bauer, B.; Lapp, A. *Macromolecules* **1985**, *18*, 986.
(22) Russell, T. P.; Hjelm, R. P., Jr.; Seeger, P. A. *Macromolecules* **1990**, *23*, 890.
(23) Russell, T. P. *Macromolecules* **1993**, *26*, 5819.
(24) Stühn, B. *J. Polym. Sci., Polym. Phys. Ed.* **1992**, *30*, 1013.
(25) Fernandez, M. L.; Higgins, J. S.; Penfold, J.; Ward, R. C.; Shackleton, C.; Walsh, D. J. *Polymer* **1988**, *29*, 1923.
(26) Higashida, N.; Kressler, J.; Yukioka, S.; Inoue, T. *Macromolecules* **1992**, *25*, 5259.
(27) Kressler, J.; Higashida, N.; Shimomai, K.; Inoue, T.; Ougizawa, T. *Macromolecules* **1994**, *27*, 2448.
(28) Callaghan, T. A.; Paul, D. R. *Macromolecules* **1993**, *26*, 2439.
(29) Helfand, E.; Tagami, Y. *J. Chem. Phys.* **1971**, *56*, 3592.
(30) Broseta, D.; Fredrickson, G. H.; Helfand, E.; Leibler, L. *Macromolecules* **1990**, *23*, 132.
(31) Flory, P. J. *Principles of Polymer Chemistry*; Cornell University Press: Ithaca, NY, 1953.
(32) Sanchez, I. C.; Lacombe, R. H. *Polym. Lett.* **1977**, *15*, 71.
(33) Flory, P. J.; Orwell, R. A.; Vrij, A. *J. Am. Chem. Soc.* **1964**, *86*, 3507.
(34) Dee, G. T.; Walsh, D. J. *Macromolecules* **1988**, *21*, 811.
(35) Amsel, G.; Nadai, J. P.; D'Artemare, E.; David, D.; Girard, E.; Moulin, J. *Nucl. Inst. Methods* **1971**, *92*, 481.
(36) Pronko, P. P. *J. Nucl. Mater.* **1974**, *53*, 252.
(37) Altstetter, C. J.; Behrisch, R.; Bøttiger, J.; Pohl, F.; Scherzer, B. M. U. *Nucl. Inst. Methods* **1978**, *149*, 59.
(38) Payne, R. S.; Clough, A. S.; Murphy, P.; Mills, P. J. *Nucl. Inst. Methods Phys. Res.* **1989**, *B42*, 130.
(39) Chaturvedi, U. K.; Steiner, U.; Zak, O.; Krausch, G.; Schatz, G.; Klein, J. *Appl. Phys. Lett.* **1990**, *56*, 1228.
(40) Crank, J. *The Mathematics of Diffusion*, 2nd ed.; Oxford University Press: Oxford, U.K., 1975.
(41) Composto, R. J.; Kramer, E. J.; White, D. M. *Macromolecules* **1988**, *21*, 2580.
(42) Budkowski, A.; Steiner, U.; Klein, J.; Schatz, G. *Europhys. Lett.* **1992**, *18*, 705.
(43) Ferry, J. D. *Viscoelastic Properties of Polymers*, 3rd ed.; Wiley: New York, 1980; pp 276−8.
(44) Kim, E.; Kramer, E. J.; Osby, J. O. *Macromolecules* **1995**, *28*, 1979.
(45) Kanetakis, J.; Fytas, G. *J. Chem. Phys.* **1987**, *87*, 5048.
(46) Meier, G.; Fytas, G.; Momper, B.; Fleischer, G. *Macromolecules* **1993**, *26*, 5310.
(47) Akcasu, A. Z.; Nägele, G.; Klein, R. *Macromolecules* **1991**, *24*, 4408.
(48) Brereton, M. P. *Prog. Colloid Polym. Sci.* **1993**, *91*, 8.
(49) Akcasu, A. Z.; Nägele, G.; Klein, R. *Macromolecules* **1995**, *28*, 6680.
(50) Feng, Y.; Han, C. C.; Takenada, M.; Hashimoto, T. *Polymer* **1992**, *33*, 2729.

MA960458E